

# The Absorption of Gamma Ray by Matter

Eric Reichwein  
David Steinberg  
Department of Physics  
University of California, Santa Cruz

August 30, 2012

## Abstract

To observe how gamma ray radiation produced by cesium-137 ( $\text{Cs}^{137}$ ) interacts with matter we placed varying thickness sheets of lead on top of the  $\text{Cs}^{137}$  source. We first determined the background radiation in the laboratory to be 0.686 counts per second. Due to Compton scattering a thin lead shielding can actually increase the amount of radiation. With no lead shielding at a fixed distance of 40mm away from the  $\text{Cs}^{137}$ , we observed a count rate of 7.6216 counts per second but with 0.9mm thick lead shielding we observed count rate of 8.086727 counts per second. By increasing the lead shielding thickness even more we observed an exponentially decreasing count rate. From the intensity versus lead thickness curve we determined the coefficient of absorption to be  $1.249\text{cm}^{-1}$ . This put the initial energy of the gamma ray emitted by the  $\text{Cs}^{137}$  at 0.6325MeV.

# Contents

<b>1</b>	<b>Introduction</b>	<b>2</b>
<b>2</b>	<b>Preliminary Experiment</b>	<b>3</b>
2.1	Number of Electrons for Each Pulse Count of GM Tube . . . . .	3
2.2	Measuring the Counting Rate . . . . .	4
2.2.1	Background Radiation Intensity . . . . .	4
2.3	Poisson Distribution of Intensity of Radiation from a Radioactive Source . . . . .	5
2.4	The Counter Dead Time . . . . .	6
2.4.1	Effeciency of Counter . . . . .	7
<b>3</b>	<b>Absorption of Gamma Rays by Lead</b>	<b>8</b>
3.1	Z-Shielding . . . . .	8
3.2	Leads Coefficient of Absorption . . . . .	9
3.3	Dependence of $\mu$ on Gamma Ray Energy . . . . .	10
<b>4</b>	<b>Conclusion</b>	<b>12</b>
<b>A</b>	<b>Error Analysis</b>	<b>12</b>
A.1	Error in Dead time . . . . .	12
A.2	Error in Coefficient of Absorption . . . . .	13
A.2.1	Standard Deviation of Count Rate and Background Radiation Intensity . .	13
A.2.2	Propagating Error in Count Rate and Background Radiation Intensity . .	13
A.2.3	Error in the Intensity . . . . .	13

## 1 Introduction

The  $Cs^{137}$  can produces two different energy beta particles. One beta particle has energy 0.5120MeV and causes the  $Cs^{137}$  to decay to  $Ba^{137}$  in an excited state; which subsequently decays to a lower energy state by emitting a 0.662MeV photon. The other beta particle has energy 1.174MeV and causes the  $Cs^{137}$  to decay directly to the non-excited  $Ba^{137}$ .

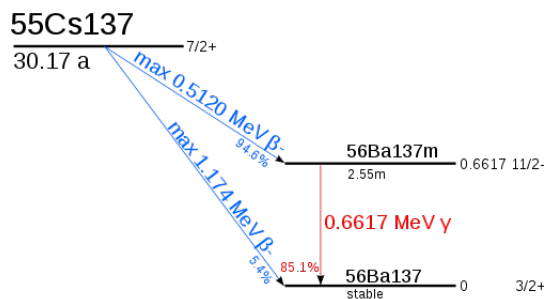


Figure 1: The  $Cs^{137}$  decay chain.[5]

There are three main ways that gamma rays interact with matter. The first way is electron-positron pair production. However, the gamma rays produced by  $Cs^{137}$  are 0.662MeV and the threshold for pair production is 1.022MeV, hence we do not take into account this interaction. Refer to Table 5 for details.

The next interaction that could occur between matter and gamma rays is the photoelectric effect. The gamma ray would hit a atom and liberate an electron. The work function lead is roughly 4eV [1], so the energy of the resulting photo-electron emitted is given by Einsteins Famous equation

$$E_{PE} = E_{\gamma} - \phi_{Lead}$$

This would put the resulting photo-electron in the category of a beta particle. This interaction could decrease or have no affect on the number of counts due to scattering, but never increase the number of counts.

The last type of interaction is Compton scattering which could produce a high energy electron (beta particle) and a slightly less energetic gamma ray. This type of interaction is characterized by Author Compton’s famous equation

$$\lambda'_{\gamma} - \lambda_{\gamma} = \frac{h}{m_0c} (1 - \cos(\theta))$$

Where  $\lambda_{\gamma}$  is the incident gamma ray,  $\lambda'_{\gamma}$  is the wavelength of the “scattered” photon, and  $\theta$  is the angle between the initial gamma rays trajectory and the “scattered” gamma ray. For certain angles this interaction could actually increase the intensity of radiation detected by the Geiger-Muller tube.

## 2 Preliminary Experiment

Before we determined the intensity as a function of shielding thickness we measured the amount charge collected on the blocking capacitor, the counting rate of the Hewlett-Packard Model 5314A counter, and the background radiation. Our setup consisted of the GM tube connected to ”scratch” filter with a high voltage source and then to the oscilloscope, as seen Figure 2.

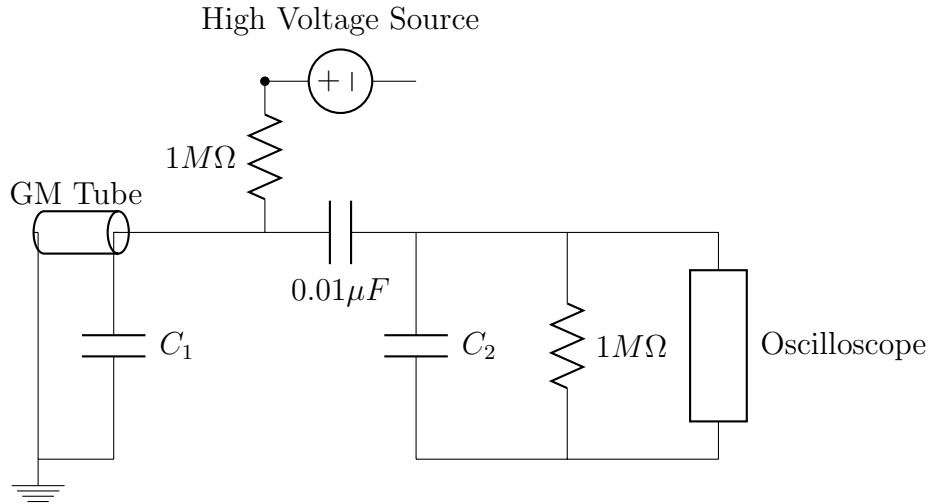


Figure 2: The Experimental setup.  $C_1$  and  $C_2$  are internal capacitance’s and are typically much less than the blocking capacitor,  $C$ . [3]

### 2.1 Number of Electrons for Each Pulse Count of GM Tube

To determine the pulse shape of each GM tube detection we measure the change in voltage across the high pass filter. In Figure 2 the oscilloscope is measuring the change in voltage across  $C$

relative to ground. The pulse shape has quick rise then a slow decay as seen the Figure 3.

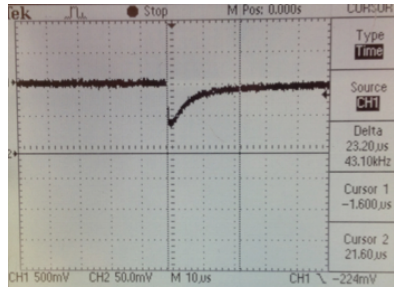


Figure 3: The shape of pulse when Geiger-Muller tube registers radiation. The high voltage supply was set at 800V.

To determine the number electrons,  $n_e$ , on the negative side of the capacitor, we use the definition of capacitance and the definition of electric charge to obtain  $n_e$

$$Q = C\Delta V \qquad Q = n_e e^- \longrightarrow n_e = \frac{Q}{e^-}$$

The change in voltage, across our  $0.01\mu F$  blocking capacitor, as the GM tube detected some form of radiation was  $0.544V$ . Hence, the total number of electrons on the capacitor is

$$n_e = \frac{C\Delta V}{e^-} = \frac{0.01\mu F \times 0.544V}{1.60217646 \times 10^{-19}C} = 3.4 \times 10^{10} \text{ electrons}$$

## 2.2 Measuring the Counting Rate

We determined, by trial and error, that the front window of the GM tube was the most sensitive part of the GM tube to radiation. We also determined that one side of the  $Cs^{137}$  source emits more radiation per second than the other. To measure the maximum counting rate we placed the most sensitive part of the GM tube as close as possible to the more active side of the  $Cs^{137}$  source. We detected a total of 16,033 radioactive particles in 22.07 seconds. The maximum counting rate was determined to be

$$\text{Maximum Counting Rate} = \frac{\text{Total Counts}}{\text{Total Time}} = \frac{16,033\text{counts}}{22.07\text{s}} = 726 \frac{\text{counts}}{\text{sec}}$$

Finally, we investigated the plateau region of the GM Tube. We found that the area between 800V and 950V did not significantly alter the counts per second. However, when we dropped the voltage below 800V we noticed a steep decline in counts per second.

### 2.2.1 Background Radiation Intensity

We determined the background counting rate by first removing all radioactive sources from the laboratory. Then we positioned the GM tube downwards, just as in the rest of the experiment. Then let the counter go for 25 minutes. We measured a total of 1029 hits. This gave us a background counting rate of 0.686 counts per second.

## 2.3 Poisson Distribution of Intensity of Radiation from a Radioactive Source

We placed the Cs<sup>137</sup> approximately 40mm below the window of the GM Tube and observed a count rate that varied between 5 counts per second to 10 counts per second. By using a video camera and the Hewlett-Packard Counter we were able to accurately determine the number of counts per second. We started the counter first and then begin recording after 100 seconds we stopped recording. We parsed through the video in one second intervals and recorded the number of counts. Table 1 shows the number number one second intervals in the first column, total number of counts in the second column, and number of counts in the third column. The three columns then repeat three more times to show all 100 one second intervals.

#	total counts, N	$\Delta N$	#	N	$\Delta N$	#	N	$\Delta N$	#	N	$\Delta N$
1	173	4	26	319	3	51	457	4	76	619	5
2	177	6	27	322	1	52	461	1	77	624	8
3	183	3	28	323	5	53	462	5	78	632	6
4	186	9	29	328	7	54	467	12	79	638	5
5	195	5	30	335	5	55	479	11	80	643	4
6	200	5	31	340	3	56	490	9	81	647	5
7	205	4	32	343	8	57	499	5	82	652	6
8	209	6	33	351	8	58	504	4	83	658	6
9	215	3	34	359	9	59	508	7	84	664	4
10	218	8	35	368	3	60	515	5	85	668	2
11	226	6	36	371	5	61	520	3	86	670	4
12	232	5	37	376	5	62	523	5	87	674	6
13	237	9	38	381	7	63	528	10	88	680	6
14	246	2	39	388	5	64	538	1	89	686	9
15	248	4	40	393	5	65	539	9	90	695	4
16	252	10	41	398	4	66	548	10	91	699	7
17	262	4	42	402	9	67	558	8	92	706	3
18	266	7	43	411	6	68	566	5	93	709	9
19	273	10	44	417	5	69	571	7	94	718	5
20	283	3	45	422	7	70	578	10	95	723	4
21	286	11	46	429	7	71	588	8	96	727	3
22	297	5	47	436	7	72	596	7	97	730	7
23	302	5	48	443	4	73	603	4	98	737	3
24	307	4	49	447	4	74	607	6	99	740	8
25	311	8	50	451	6	75	613	6	100	748	4

Table 1: The 100 one second intervals for radioactive decay particles given off by Cs<sup>137</sup>. The GM Tube was placed approximately 40mm above the Cs<sup>137</sup>.

By applying built-in functions of the CERN open source data analysis program ROOT, we were able to determine  $\chi^2$  for our histogram of the count rates (counts per second) to be 6.373.

We found our mean value for the count rate to be 5.73 counts per second. Since we took 100 measurements we can say that

$$\bar{m} = \sum_0^{100} mP(m) \approx \sum_0^{\infty} mP(m) = \lambda$$

We had 5 degrees of freedom ( $\nu = 5$ ), and  $\chi^2 = 6.373$  giving  $\frac{\chi^2}{\nu} = 1.2746$ . Using the “goodness of fit” test we determined our  $\alpha$  to be  $.6926 \pm 0.1534$ , which is  $p2$  in Figure 4. This value is close to 0.5, which means our Poisson distribution is a reasonable one. The error on our  $\alpha$  would put our  $\alpha$  value close to 0.5 which furthers our confidence of our Poisson distribution.

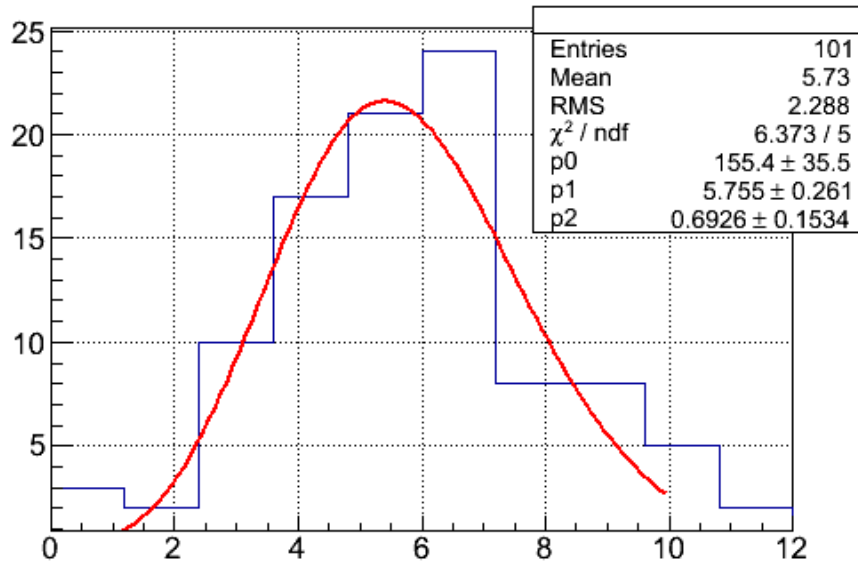


Figure 4: Poisson distribution of radiation intensity

## 2.4 The Counter Dead Time

The GM tube will be disabled for a brief period after it detects some form of radiation. We refer to this disabled time period as the dead time,  $\tau$ . It can be shown that the dead is equal to [3]

$$\tau = \frac{1}{n_{ab}} \left\{ 1 - \left[ 1 - \frac{n_{ab}(n_a + n_b - n_{ab})}{n_a n_b} \right]^{\frac{1}{2}} \right\} \quad (1)$$

Where  $n_a$ ,  $n_b$ , and  $n_{ab}$  are the number of pulses seen by the oscilloscope that are registered, by radioactive source a, b and both sources combined, respectively. We used two Cs<sup>137</sup> sources placed as close as possible to the GM tube to obtain the values in Table 2. We used the average value of the number of counts for each source and both sources combined in Equation 1.

$n_a$	$n_b$	$n_{ab}$	$\sigma_{n_a}$	$\sigma_{n_b}$	$\sigma_{n_{ab}}$
551	618	966	-17.2	6	-3
524	639	957	9.8	-15	6
518	626	986	15.8	-2	-23
554	596	933	-20.2	28	30
522	641	973	11.8	-17	-10
Average	Average	Average	Sum	Sum	Sum
533.8	624	963	$\approx 0$	0	0

Table 2: The counting rate for two different  $\text{Cs}^{137}$  sources and both of the  $\text{Cs}^{137}$  sources together.

Our predicted value for the dead time,  $\tau_{pred}$ , is  $350\mu\text{s}$ . Our measured value for the dead time with one source,  $\tau_1$ , was  $440\mu\text{s}$ . With two sources we measured our dead time,  $\tau_2$ , to be  $290\mu\text{s}$ . It turns out that the the average of these two dead times,  $\overline{\tau_{12}}$ , is  $365\mu\text{s}$ , which is very close to our predicted value,  $\tau_{pred}$ .

By using error propagation techniques described in the appendix, we derived a standard deviation for the predicted dead time of  $116\mu\text{s}$ , which gives a dead time of

$$\tau = 350 \pm 116\mu\text{s}$$

This large error shows the true statistical uncertainty of nature and electronic equipment. However, this large error puts our measured dead times within reason. The characteristic dead time signal is shown below in Figure 5.

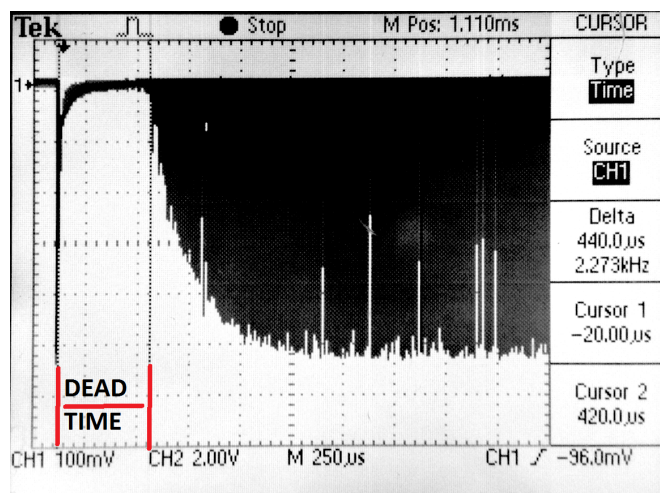


Figure 5: The oscilloscope reading the change in voltage across the blocking capacitor during high radiation intensity detection.

### 2.4.1 Efficiency of Counter

The number of total particles,  $m$ , passing through the detector is given by [3]

$$m = \frac{n}{1 - n\tau}$$

Where  $n$  is the number particles registered by the detector. To get the efficiency of the counter due to the effect of the dead time we simply take the ratio of number of registered particles to total number of particles

$$\frac{n}{m} = \frac{n}{\frac{n}{1-n\tau}} = 1 - n\tau$$

The lowest efficiency would be at the highest counting rate which would be 8.086 for our experiment. This would have an efficiency of 99.7%. The dead time for our experiment has little effect on the results, since the intensity of radiation is relatively small. The efficiency at the maximum possible count rate, 726 counts per second, is only 75%. This means all the measurements we took were at least 99.7%.

### 3 Absorption of Gamma Rays by Lead

#### 3.1 Z-Shielding

The Z-shielding is three-layer shielding consisting of tantalum, tin, and steel. It is called graded Z-shielding since it has a grade of atomic number(s) from highest to lowest, or vice versa. Depending on what atomic number your shielding material is you will get different shielding results and effects. For the graded Z-shielding the larger atomic number layer absorbs gamma rays more readily through various interactions, including X-ray fluorescence and Brehmsstrahlung radiation. It also “absorbs” electrons more readily through an increase in Coulomb scattering. If the radiation hits the least dense side first it will scatter and effectively lower the energy of the reflected radiation. The scattered lower energy gamma rays (or X-rays) then get absorbed more readily by the following denser shielding layers [2]. It is essential like stopping a car, you start by applying a little brake then gradually applying more brake to make a complete nice stop.

Graded Z-shield configuration	counts	time	expected back-ground (bg)	counts-bg	counts per second
Steel up+.9mm	1000	148.0s	101.5s <sup>-1</sup>	898.472	6.07075676s <sup>-1</sup>
Steel down+.9mm	1009	133.9s	91.9s <sup>-1</sup>	917.1446	6.84947424s <sup>-1</sup>
Steel up	1001	119.2s	81.8s <sup>-1</sup>	919.2288	7.71165101s <sup>-1</sup>
Steel down	1001	124.6s	85.5s <sup>-1</sup>	915.5244	7.34770787s <sup>-1</sup>

Table 3: The counting rate with the three metal shielding. Z-shield is 1mm thick and consists of one layer of tantalum, one layer of tin, and one layer of steel. The GM tube is placed 40mm above the Cs<sup>137</sup> source. The density of steel is 7.85kg/cm<sup>3</sup>, tin is 6.99kg/cm<sup>3</sup>, and tantalum is 16.65kg/cm<sup>3</sup>.

Table 3 shows what we predicted the thicker the shielding the less radiation that gets through. It also shows that you get less radiation passing through the graded Z-shielding if it is placed from lowest atomic number to highest.



### 3.2 Leads Coefficient of Absorption

To determine the coefficient of absorption of lead we placed the GM tube 40mm above the Cs<sup>137</sup> source, and placed an increasing amount of lead between the source and the GM tube. We expected to see a slight increase when placing a thin sheet of lead on top of the Cs<sup>137</sup> source due to Compton scattering. Compton Scattering as seen in the Figure 5 produces a high energy beta particle and a lower energy gamma ray if the scattering angles are small. This would give us an increased count rate if the lead shielding is thin. If the lead were not thin the beta particle would be severely affected by Coulomb scattering. This relatively thin lead piece of shielding actually produces more radiation than if it were not there at all because the electron ejected by Compton scattering has very few chances to be affected by Coulomb scattering.

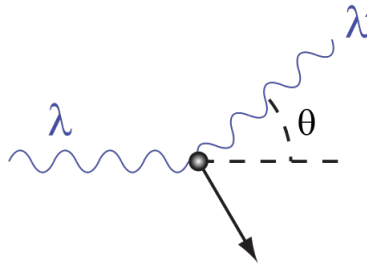


Figure 6: Diagram of Compton scattering.[6]

Figure 6 shows a diagram of Compton scattering. For small angles of scattering both the ejected electron and scattered gamma ray can have the right trajectories and energies to be detected by the GM tube. However, after some thickness (approximately 1mm) of lead the intensity of radiation getting through the lead decreases exponentially, the intensity is given as function thickness of the shielding material

$$I(t) = I_0 e^{-\mu x} \quad (2)$$

Where  $\mu$  is Coefficient of Absorption and  $x$  is the thickness of the material. Table 4 shown below is the data for the intensity versus lead thickness. Just as we expected there was a slight increase in intensity as we placed the 0.9mm thick lead sheet over the Cs<sup>137</sup>, and an exponential decrease in intensity as we increased the lead thickness.

Lead Thickness	counts	time	expected back-ground (bg)	counts-bg	counts per second
0mm	1350	162.5s	111.475	1238.525	7.62169231
0.9mm	1158	132s	90.552	1067.448	8.08672727
6.0mm	1002	204s	139.944	862.056	4.22576471
11.1mm	1010	332.6s	228.1636	781.8364	2.3506807
16.2mm	1000	519s	356.034	643.966	1.24078227
21.2mm	1001	740.6s	508.0516	492.9484	0.66560681
26.2mm	1000	1098.7s	753.7082	246.2918	0.22416656
31.3mm	1000	1602.8s	1099.5208	-99.5208	-0.0620918

Table 4: The Lead Thickness and counting rate of radiation of the GM tube 4cm above Cs<sup>137</sup>

To determine the Coefficient of Absorption of lead we find the straight line fit to natural log of the intensity function

$$\ln(I) = \ln(I_0) - \mu x \quad (3)$$

Now the resulting line has a slope that is equal to the Coefficient of Absorption,  $\mu$ , of lead. Figure 7 shows the line characterized by Equation 2. According to Table 6, our Coefficient of Absorption is within the energy range of the gamma ray produced by Cs<sup>137</sup>. Our straight line fit passes through every point except the point with 31.3mm thick lead shielding. The reason we believe it does not pass through the last point is that the lead may have been blocking some background radiation since it was so close to GM tube. The 31.3mm of lead stacked up to about 36mm tall due to uneven surface of lead. Multiple factors could contribute to the last data point having observed negative intensity, so we considered it just background radiation. The value of our Coefficient of Absorption,  $\mu$ , is found Figure 7 as  $p0$  and is given as

$$\mu = 1.249 \pm 0.02781 \text{cm}^{-1}$$

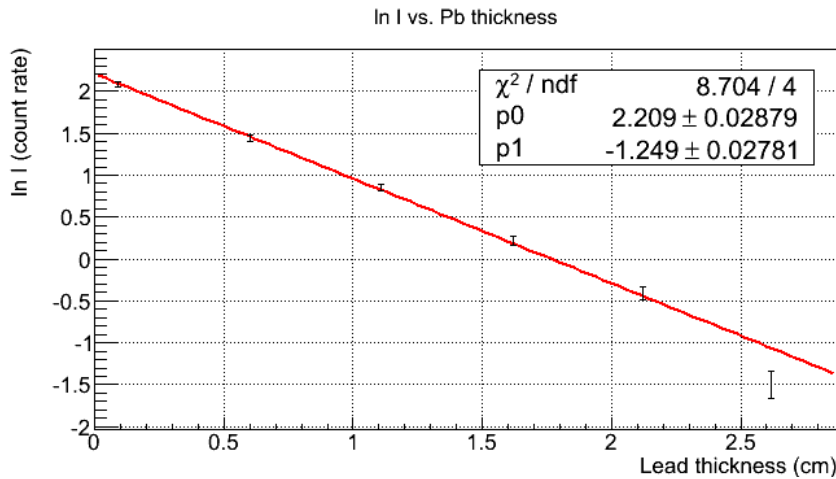


Figure 7: Photon energy vs. Thickness of Lead.

If we consider our efficiency due to dead time we see a very slight increase in our increase confidence level,  $\alpha$ , and a  $\mu$  value that would give reconstructed gamma ray energy closer to the theoretical energy of 0.662MeV. However, it would only change our presented values by a fraction of a percent so we have omitted the calculations and resulting graph. Our model predicts an initial photon energy of 0.6325MeV.

### 3.3 Dependence of $\mu$ on Gamma Ray Energy

By plotting the data in Table 6 we were able to obtain a relation between  $\mu$  and photon energy. Extrapolating from this graph with our predicted value of  $\mu$ , we determined that the gamma ray energy released from the Cs<sup>137</sup> is 0.6325MeV. Comparing to the predicted gamma ray emitted from the nuclear de-excitation of Ba<sup>137</sup> of 0.662MeV.

Photon Energy (MeV)	Photo electric $\sigma_{PE}$	Compton $\sigma_C$	Pair For- mation $\sigma_{PF}$	Total $\sigma_T$	Coeffecient per cm $\mu$ , $cm^{-1}$	Mass Co- efficient $\frac{\mu}{\rho} \frac{cm^2}{gm}$
0.1022	1782	40.18		1822	59.9	5.3
0.1277	985	38.01		1023	33.6	2.97
0.1703	465	35.04		500	16.4	1.45
0.2554	161	30.7		192	6.31	0.558
0.3405	75.7	27.63		103.3	3.39	0.3
0.4086	47.8	25.74		73.5	2.42	0.214
0.5108	27.7	23.5		51.2	1.68	0.149
0.6811	14.5	20.73		35.2	1.16	0.102
1.022	6.31	17.14		23.45	0.771	0.0682
1.362	3.86	14.81	0.1948	18.87	0.62	0.0549
1.533		13.91	0.3313			
2.043	2.08	11.86	1.247	15.19	0.499	0.0442
2.633						
3.065		9.313	3.507			
4.086	0.369	7.761	5.651	14.28	0.469	0.0415
5.108	0.675	6.698	7.56	14.93	0.491	0.0434
6.13		5.917	9.119			
10.22	0.316	4.115	14.04	18.47	0.607	0.0537
15.32	0.206	3.042	18	21.25	0.698	0.0618
25.54	0.122	2.044	23.24	25.41	0.835	0.0739

Table 5: Values of the Absorption Coefficient for Lead ( $10^{-24}cm^2/atom$ ).

The logarithm plot of column one versus column 6 of Table 5 is shown below. From this graph we determined our predicted gamma ray energy.

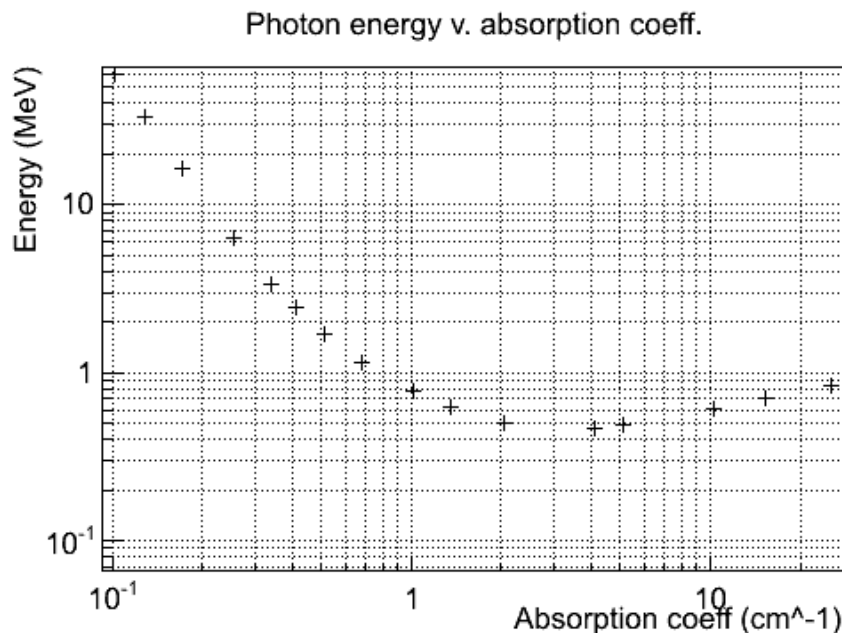


Figure 8: Photon energy vs. Absorption Coefficient.

## 4 Conclusion

Many factors go into the rate of absorption of gamma rays by lead. By using elementary quantum mechanics we were able to determine the rate at which lead absorbs gamma rays, which includes the processes of Compton scattering and photoelectric effect. Electron-positron pair formation also factors in but not with the photon energies we used in this experiment. We also determined that choosing the right thickness of shielding is important because if the shielding is too thin it could actually increase the amount of radiation due to Compton scattering.

## A Error Analysis

To obtain the results in table 6 we used the partial derivative method of error propagation [4]

$$\sigma_f^2 = \frac{1}{N} \sum_{i=1}^N \left( \frac{\partial f}{\partial x_i} \right)^2 \sigma_i^2 \quad (4)$$

To obtain the average standard deviation of multiple measurements we use

$$\frac{1}{\sigma^2} = \sum_{i=1}^N \frac{1}{\sigma_i^2}$$

### A.1 Error in Dead time

We first found the standard deviation of each individual measurement subtracting each measurement from its average value. The standard deviations for each value  $n_a$ ,  $n_b$ , and  $n_{ab}$  are found in

Table 2. We then calculated the derivatives of Equation 1 as

$$\begin{aligned}\frac{d\tau}{dn_a} &= \frac{\sqrt{\frac{(n_a-n_{ab})(n_b-n_{ab})}{n_a n_{ab}}}}{2n_a(n_a-n_b)} \\ \frac{d\tau}{dn_b} &= \frac{\sqrt{\frac{(n_a-n_{ab})(n_b-n_{ab})}{n_a n_b}}}{2n_b(n_b-n_{ab})} \\ \frac{d\tau}{dn_{ab}} &= \frac{-n_a \left( 2n_b \left( \sqrt{\frac{(n_a-n_{ab})(n_b-n_{ab})}{n_a n_b}} - 1 \right) + n_b \right) - n_b n_{ab}}{2n_a n_b n_{ab}^2 \sqrt{\frac{(n_a-n_{ab})(n_b-n_{ab})}{n_a n_b}}}\end{aligned}$$

Using the values from Table 2 and Equation 4 we find that the standard deviation of the dead time with accurate error propagation is  $\pm 116 \mu\text{s}$ .

## A.2 Error in Coefficient of Absorption

We used the same error propagation techniques as seen in previous section in determining the standard deviation of  $\mu$ . The population variance  $\nu^2 = \lambda$  where  $\lambda$  is the average number of counts.[3] By isolating  $\mu$  we obtain

$$\mu = -\frac{\ln\left(\frac{I}{I_0}\right)}{x}$$

The results of the error propagation using the technique of Equation 3 and Equation 4 is shown in Table 6. Column 1 is just the natural log the last column of Table 4. Since we are going to to taking a ratio of intensities we can assume the counting rate is the intensity.

### A.2.1 Standard Deviation of Count Rate and Background Radiation Intensity

The counting rate standard deviation,  $\sigma_c$ , and background standard deviation is given as

$$\sigma = \frac{\sqrt{N}}{t}$$

Where  $N$  is the total number of counts and  $t$  is the amount of time to acquire that amount of counts. These errors are shown in columns 2 and 3 of Table 6.

### A.2.2 Propagating Error in Count Rate and Background Radiation Intensity

To propagate the error in the measurements through we square both and add them in quadrature. The value for the propagated error of our measurements are shown in column 4 of Table 6.

$$\sigma_{\text{BG+C}} = \sqrt{\sigma_{\text{BG}}^2 + \sigma_{\text{C}}^2}$$

### A.2.3 Error in the Intensity

The intensity of the  $\text{Cs}^{137}$  is given by  $I = I_C - I_{\text{BG}}$ . Using the derivative method we first calculate the derivatives of the intensity function

$$\frac{d}{dI_C} \ln I = \frac{1}{I_C - I_{\text{BG}}} \qquad \frac{d}{dI_{\text{BG}}} \ln I = \frac{-1}{I_C - I_{\text{BG}}}$$

Applying Equation 4 we find

$$\begin{aligned}\sigma_{\ln I}^2 &= \left(\frac{d}{dI_C} \ln I\right)^2 \sigma_C^2 + \left(\frac{d}{dI_{BG}} \ln I\right)^2 \sigma_{BG}^2 \\ \sigma_{\ln I}^2 &= \left(\frac{1}{I_C - I_{BG}}\right)^2 \sigma_C^2 + \left(\frac{-1}{I_C - I_{BG}}\right)^2 \sigma_{BG}^2 \\ \sigma_{\ln I}^2 &= \frac{\sigma_C^2}{(I_C - I_{BG})^2} + \frac{\sigma_{BG}^2}{(I_C - I_{BG})^2} \\ \sigma_{\ln I}^2 &= \frac{\sigma_{BG}^2 + \sigma_C^2}{(I_C - I_{BG})^2}\end{aligned}$$

Then taking the square root of both sides we get a standard deviation of the natural log of intensity to be

$$\sigma_{\ln I} = \pm \frac{\sqrt{\sigma_{BG}^2 + \sigma_C^2}}{(I_C - I_{BG})}$$

The standard deviations of the natural log of the intensities we measured are found in the last column of Table 6.

$\ln(I)$	$\sigma_c$	$\sigma_{bg}$	$\sigma_{bg+c}$	$\sigma_{\ln(bg+c)}$
2.03099843	0.22610675	0.02138535	0.22711582	0.029798607
2.09022411	0.25779848	0.02138535	0.25868395	0.031988708
1.44120024	0.15516855	0.02138535	0.15663528	0.03706673
0.85470494	0.09555171	0.02138535	0.09791558	0.04165414
0.21574205	0.06093021	0.02138535	0.06457417	0.052043109
-0.4070562	0.04272021	0.02138535	0.04777394	0.071775014
-1.4953659	0.02878199	0.02138535	0.03585717	0.159957694
N/A	0.01972971	0.02138535	0.0290963	-0.468601009

Table 6: Standard deviation propagation in determining  $\mu$ .

## References

- [1] P. A. Anderson and A. L. Hunt. Work function of lead. *Physical Review*, 102:367–368, April 1956.
- [2] W.C. Fan, C.R. Drumm, S.B. Roeske, and G.J. Scrivner. Shielding considerations for satellite microelectronics. *Nuclear Science, IEEE Transactions on*, 43(6):2790–2796, dec 1996.
- [3] Fred Kuttner and George Brown. *Physics 133*, 2012.
- [4] Louis Lyons. *A practical guide to data analysis for physical science students*, 1991.
- [5] Ervin B. Podgorsak. *Modes of radioactive decay*, 2010.
- [6] Wikipedia. Compton scattering — Wikipedia, the free encyclopedia, 2004. [Online; accessed 8-August-2012].